
First Order Optimization in Policy Space for Constrained Deep Reinforcement Learning

Yiming Zhang¹ Quan Vuong² Keith W. Ross^{3,1}

Abstract

In reinforcement learning, an agent attempts to learn high-performing behaviors through interacting with the environment, such behaviors are often quantified in the form of a reward function. However some aspects of behavior, such as ones which are deemed unsafe and are to be avoided, are best captured through constraints. We propose a novel approach called First Order Constrained Optimization in Policy Space (FOCOPS) which maximizes an agent’s overall reward while ensuring the agent satisfies a set of cost constraints. Using data generated from the current policy, FOCOPS first finds the optimal update policy by solving a constrained optimization problem in the nonparameterized policy space. FOCOPS then projects the update policy back into the parametric policy space. Our approach provides a guarantee for constraint satisfaction throughout training and is first-order in nature therefore extremely simple to implement. We provide empirical evidence that our algorithm achieves better performance on a set of constrained robotics locomotive tasks compared to current state of the art approaches.

1. Introduction

In recent years, Deep Reinforcement Learning (DRL) saw major breakthroughs in several challenging high-dimensional tasks such as Atari games (Mnih et al., 2013; 2016; Van Hasselt et al., 2016; Schaul et al., 2015; Wang et al., 2017), playing go (Silver et al., 2016; 2017), and robotics (Peters & Schaal, 2008; Schulman et al., 2015a; 2017; Wu et al., 2017; Haarnoja et al., 2018). However most modern DRL algorithms allow the agent to freely explore the state and action space to obtain desirable behavior, pro-

vided that it leads to performance improvement. No regard is given to whether the agent’s behavior may lead to negative consequences that outweigh the long-term value of exploration. Consider for instance the task of controlling a robot, certain maneuvers may damage the robot, or worse harm people around the robot. RL safety (Amodei et al., 2016) is a pressing topic in modern reinforcement learning research and imperative to applying reinforcement learning to real-world settings.

Constrained Markov Decision Processes (CMDP) (Kallenberg, 1983; Ross, 1985; Beutler & Ross, 1985; Ross & Varadarajan, 1989; Altman, 1999) provide a principled mathematical framework for dealing with such problems as it allows us to naturally incorporate safety criteria in the form of constraints. In low-dimensional finite settings, an optimal policy for CMDPs with known dynamics can be found by linear programming (Kallenberg, 1983) or Lagrange relaxation (Ross, 1985; Beutler & Ross, 1985).

While we can solve problems with small state and action spaces via linear programming and value iteration, function approximation is required in order to generalize over large state spaces. Chow et al. (2017) and Tessler et al. (2018) extended traditional Lagrange relaxation techniques to use function approximation. Alternatively, Achiam et al. (2017) proposed the Constrained Policy Optimization (CPO) algorithm based on local policy search methods (Kakade & Langford, 2002; Peters & Schaal, 2008; Schulman et al., 2015a). CPO approximately updates the policy to satisfy constraint with a theoretical guarantee for performance improvement and constraint satisfaction within a trust region framework.

However policy updates for the CPO algorithm involve solving an optimization problem through Taylor approximations and inverting a high-dimensional Fisher information matrix. These approximations often result in infeasible updates which would require additional recovery steps, this could sometimes cause updates to be backtracked leading to a waste of samples.

In this paper, we propose the First Order Constrained Optimization in Policy Space (FOCOPS) algorithm. FOCOPS attempts to answer the following question: given some cur-

¹New York University, NY, U.S.A. ²University of California San Diego, CA, U.S.A. ³New York University Shanghai, Shanghai, China. Correspondence to: Yiming Zhang <yiming.zhang@cs.nyu.edu>.

rent policy, what is the best policy update we can achieve which improves the agent’s performance while satisfying the cost constraint bounds at the same time? FOCOPS provides a solution to this question in the form of a two-step approach. First, we will show that the best policy update has a near-closed form solution when attempting to solve for the optimal policy in the nonparametric policy space rather than the parameter space. However in most cases, this optimal policy is impossible to evaluate. Hence we project this policy back into the parametric policy space. This can be achieved by drawing samples from the current policy and evaluating a loss function measuring a divergence measure between the parameterized policy and the optimal policy we found in the nonparametric policy space. Theoretically, FOCOPS has an approximate upper bound for worst-case constraint violation throughout training. Practically, FOCOPS is extremely simple to implement since it only utilizes first order approximations. We further tested our algorithm on a series of challenging high-dimensional continuous control tasks and found that FOCOPS achieves better performance while maintaining approximate constraint satisfaction compared to current state of the art approaches, in particular second-order approaches such as CPO.

2. Preliminaries

2.1. Constrained Markov Decision Process

Consider a Markov Decision Process (MDP) (Sutton & Barto, 2018) denoted by the tuple $(\mathcal{S}, \mathcal{A}, R, P, \mu)$ where \mathcal{S} is the state space, \mathcal{A} is the action space, $P : \mathcal{S} \times \mathcal{A} \times \mathcal{S} \rightarrow [0, 1]$ is the transition kernel, $R : \mathcal{S} \times \mathcal{A} \rightarrow \mathbb{R}$ is the reward function, $\mu : \mathcal{S} \rightarrow [0, 1]$ is the initial state distribution. Let $\pi = \{\pi(a|s) : s \in \mathcal{S}, a \in \mathcal{A}\}$ denote a policy, and Π denote the set of all stationary policies. We aim to find a stationary policy that maximizes the expected discount return which is defined as:

$$J(\pi) := \mathbb{E}_{\tau \sim \pi} \left[\sum_{t=0}^{\infty} \gamma^t R(s_t, a_t) \right]. \quad (1)$$

Here $\tau = (s_0, a_0, \dots)$ is a sample trajectory and $\gamma \in (0, 1)$ is the discount factor. We use $\tau \sim \pi$ to indicate that the trajectory distribution depends on π where $s_0 \sim \mu$, $a_t \sim \pi(\cdot|s_t)$, and $s_{t+1} \sim P(\cdot|s_t, a_t)$. We express the value function V^π and action-value function Q^π as

$$V^\pi(s) := \mathbb{E}_{\tau \sim \pi} \left[\sum_{t=0}^{\infty} \gamma^t R(s_t, a_t) \middle| s_0 = s \right] \quad (2)$$

$$Q^\pi(s, a) := \mathbb{E}_{\tau \sim \pi} \left[\sum_{t=0}^{\infty} \gamma^t R(s_t, a_t) \middle| s_0 = s, a_0 = a \right] \quad (3)$$

The advantage function is $A^\pi(s, a) := Q^\pi(s, a) - V^\pi(s)$. Finally, we define the discounted future state distribution as:

$$d^\pi(s) := (1 - \gamma) \sum_{t=0}^{\infty} \gamma^t P(s_t = s | \pi). \quad (4)$$

A Constrained Markov Decision Process (CMDP) (Kallenberg, 1983; Ross, 1985; Beutler & Ross, 1985) is an MDP with an additional set of constraints \mathcal{C} which restricts the set of allowable policies. The set \mathcal{C} consists of a set of cost functions $C_i : \mathcal{S} \times \mathcal{A} \rightarrow \mathbb{R}$, $i = 1, \dots, m$. Define the expected discounted return of policy π w.r.t. cost function C_i as

$$J_{C_i}(\pi) := \mathbb{E}_{\tau \sim \pi} \left[\sum_{t=0}^{\infty} \gamma^t C_i(s_t, a_t) \right]. \quad (5)$$

We refer to $J_{C_i}(\pi)$ as the C_i -return. The set of feasible policies is then

$$\Pi_{\mathcal{C}} := \{\pi \in \Pi : J_{C_i}(\pi) \leq b_i, i = 1, \dots, m\} \quad (6)$$

The reinforcement learning problem w.r.t. a CMDP is to find a policy such that

$$\pi^* = \operatorname{argmax}_{\pi \in \Pi_{\mathcal{C}}} J(\pi) \quad (7)$$

Analogous to the standard V^π , Q^π , and $A^\pi(s, a)$ for return, we define the cost value function, cost action-value function, and cost advantage function as $V_{C_i}^\pi$, $Q_{C_i}^\pi$, and $A_{C_i}^\pi(s, a)$ where we replace the reward R with C_i . Without loss of generality, we will restrict our discussion to the case of one constraint with a cost function C . However we will briefly discuss in later sections how our methodology can be naturally extended to the multiple constraint case.

2.2. Solving CMDPs via Local Policy Search

Typically, we update policies by drawing samples from the environment, hence we usually consider a set of parameterized policies (for example, neural networks with a fixed architecture) $\Pi_\theta = \{\pi_\theta : \theta \in \Theta\} \subset \Pi$ from which we can easily evaluate and sample from. Conversely throughout this paper, we will also refer to Π as the *nonparameterized policy space*.

Suppose we have some policy update procedure and we wish to update the policy at the k th iteration π_{θ_k} to obtain $\pi_{\theta_{k+1}}$. Updating π_{θ_k} within some local region (i.e. $D(\pi_\theta, \pi_{\theta_k}) < \delta$ for some divergence measure D) can often lead to more stable behavior and better sample efficiency (Peters & Schaal, 2008). In particular, theoretical guarantees for policy improvement can be obtained when D is chosen to be $D_{\text{KL}}(\pi_\theta || \pi_{\theta_k})$ (Kakade & Langford, 2002; Pirotta et al., 2013; Schulman et al., 2015a; Achiam et al., 2017).

However solving CMDPs directly within the context of local policy search can be challenging and sample inefficient since after each policy update, additional samples need to be

collected from the new policy in order to evaluate whether the C constraints are satisfied. Achiam et al. (2017) was able to overcome this issue by replacing the cost constraint with a surrogate cost function:

$$\tilde{J}_C(\pi_\theta) := J_C(\pi_{\theta_k}) + \frac{1}{1-\gamma} \mathbb{E}_{\substack{s \sim d^{\pi_{\theta_k}} \\ a \sim \pi_\theta}} [A_C^{\pi_{\theta_k}}(s, a)]. \quad (8)$$

This new surrogate function allows us to evaluate the constraint $J_C(\pi_\theta)$ using samples collected from the current policy π_{θ_k} . Furthermore, it can be shown that when π_θ and π_{θ_k} are close in the sense of KL-divergence, the surrogate function $\tilde{J}_C(\pi_\theta)$ is a good approximation of $J_C(\pi_\theta)$ (Achiam et al., 2017).

Using the surrogate cost constraint, Achiam et al. (2017) proposed the CPO algorithm which performs policy updates as follows: given some policy π_{θ_k} ($k = 0, 1, \dots$), the new policy $\pi_{\theta_{k+1}}$ is obtained by solving the optimization problem

$$\underset{\pi_\theta \in \Pi_\theta}{\text{maximize}} \quad \mathbb{E}_{\substack{s \sim d^{\pi_{\theta_k}} \\ a \sim \pi_\theta}} [A^{\pi_{\theta_k}}(s, a)] \quad (9)$$

$$\text{subject to} \quad \tilde{J}_C(\pi_\theta) \leq b \quad (10)$$

$$\bar{D}_{\text{KL}}(\pi_\theta \parallel \pi_{\theta_k}) \leq \delta. \quad (11)$$

where $\bar{D}_{\text{KL}}(\pi_\theta \parallel \pi_{\theta_k}) := \mathbb{E}_{s \sim d^{\pi_{\theta_k}}} [D_{\text{KL}}(\pi_\theta \parallel \pi_{\theta_k})[s]]$. We will henceforth refer to constraint (10) as the *cost constraint* and (11) as the *trust region constraint*. For policy classes with a high-dimensional parameter space such as deep neural networks, it is often infeasible to solve Problem (9-11) directly in terms of θ . Achiam et al. (2017) solves Problem (9-11) by first applying first and second order Taylor approximation to the objective and constraints, the resulting optimization problem is convex and can be solved using standard convex optimization algorithms.

However such an approach introduces several sources of error, namely (i) Sampling error resulting from taking sample trajectories from the current policy (ii) Approximation errors resulting from Taylor approximations (iii) Solving the resulting optimization problem post-Taylor approximation involves taking the inverse of a Fisher information matrix, whose size is equal to the number of parameters in the policy network. Inverting such a large matrix is computationally expensive to attempt directly hence the CPO algorithm uses the conjugate gradient method (Strang, 2007) to indirectly calculate the inverse. This results in further approximation errors. In practice the presence of these errors require the CPO algorithm to take additional steps during each update in the training process in order to recover from constraint violations, this is often difficult to achieve and may not always be work well in practice. We will show in the next several sections that our approach is able to eliminate the last two sources of error and outperform CPO using a simple first-order method.

2.3. Related Work

In the tabular setting, CMDPs have been extensively studied by the Markov Decision Process community for a wide range of different constraint criteria (Kallenberg, 1983; Beutler & Ross, 1985; 1986; Ross, 1989; Ross & Varadarajan, 1989; 1991; Altman, 1999).

In high-dimensional settings, Chow et al. (2017) proposed a primal-dual method which is shown to converge to policies satisfying cost constraints. Alternatively, Tessler et al. (2018) introduced a penalized reward formulation and used a multi-timescaled approach for training an actor-critic style algorithm which guarantees convergence to a fixed point. However multi-timescaled approaches impose stringent requirements on the learning rates which can be difficult to tune in practice. We note that neither of these methods are able to guarantee cost constraint satisfaction during training.

Recently Yang et al. (2020) independently proposed the Projection-Based Constrained Policy Optimization (PCPO) algorithm which utilized a similar two-step approach for solving the constrained RL problem. Unlike our work, PCPO first finds the policy with the maximum return by doing one TRPO (Schulman et al., 2015a) update. It then projects this policy back into the feasible cost constraint set in terms of the minimum KL divergence. This differs from our approach where we first find the optimal constraint-satisfying policy in the nonparameterized policy space, then projects it back into the parameterized policy space. While PCPO also satisfies theoretical guarantees for cost constraint satisfaction, it uses second-order approximations in both steps. FOCOPS does not rely on second-order approximations which results in a much simpler algorithm in practice. Furthermore, based on empirical results from (Yang et al., 2020), PCPO does not consistently outperform CPO.

Our work builds upon previous advances made in the field of local policy search, in particular (Schulman et al., 2015a; 2017; Vuong et al., 2019).

3. Constrained Optimization in Policy Space

Instead of solving (9-11) directly, we use a two-step approach summarized below:

1. Given policy π_{θ_k} , find an *optimal update policy* π^* by solving the optimization problem from (9-11) in the nonparameterized policy space.
2. Project the policy found in the previous step back into the parameterized policy space Π_θ by solving for the closest policy $\pi_\theta \in \Pi_\theta$ to π^* in order to obtain $\pi_{\theta_{k+1}}$.

3.1. Finding the Optimal Update Policy

In the first step, we consider the optimization problem

$$\underset{\pi \in \Pi}{\text{maximize}} \quad \mathbb{E}_{\substack{s \sim d^{\pi_{\theta_k}} \\ a \sim \pi}} [A^{\pi_{\theta_k}}(s, a)] \quad (12)$$

$$\text{subject to} \quad \tilde{J}_C(\pi) \leq b \quad (13)$$

$$\bar{D}_{\text{KL}}(\pi \parallel \pi_{\theta_k}) \leq \delta \quad (14)$$

Note that this problem is almost identical to Problem (9-11) except the parameter of interest is now the nonparameterized policy π and not the policy parameter θ . We can show that Problem (12-14) admits the following solution:

Theorem 1. For fixed $\lambda > 0$ and $\nu \geq 0$, define

$$\pi^*(a|s) := \frac{\pi_{\theta_k}(a|s)}{Z_{\lambda, \nu}(s)} e^{\frac{1}{\lambda} (A^{\pi_{\theta_k}}(s, a) - \nu A_C^{\pi_{\theta_k}}(s, a))} \quad (15)$$

where the term $Z_{\lambda, \nu}(s)$ is the partition function which ensures (15) is a valid probability distribution. If π_{θ_k} is a feasible solution, the optimal policy for (12-14) is given by (15) where λ and ν are solutions to the following optimization problem:

$$\min_{\lambda, \nu \geq 0} \lambda \delta + \nu \tilde{b} + \lambda \mathbb{E}_{\substack{s \sim d^{\pi_{\theta_k}} \\ a \sim \pi^*}} [\log Z_{\lambda, \nu}(s)] \quad (16)$$

where $\tilde{b} = (1 - \gamma)(b - \tilde{J}_C(\pi_{\theta_k}))$.

To aid in our proof of Theorem 1, we will first begin by stating the following lemma (the proof can be found in Appendix A of the supplementary materials):

Lemma 1. For fixed s , $\lambda > 0$, and $\nu \geq 0$, the solution to the optimization problem:

$$\underset{\pi}{\text{maximize}} \quad \mathbb{E}_{a \sim \pi(\cdot|s)} \left[A^{\pi_{\theta_k}}(s, a) - \nu A_C^{\pi_{\theta_k}}(s, a) - \lambda (\log \pi(a|s) - \log \pi_{\theta_k}(a|s)) \right] \quad (17)$$

$$\text{subject to} \quad \sum_a \pi(a|s) = 1 \\ \pi(a|s) \geq 0 \quad \text{for all } a \in \mathcal{A}$$

is given by (15).

We are now ready to proceed with the proof of Theorem 1.

Proof. We will begin by showing that Problem (12-14) is convex w.r.t. $\pi = \{\pi(a|s) : s \in \mathcal{S}, a \in \mathcal{A}\}$. First note that the objective function is linear w.r.t. π . Since $J_C(\pi_{\theta_k})$ is a constant w.r.t. π , constraint (13) is linear. Constraint (14) can be rewritten as $\sum_s d^{\pi_{\theta_k}}(s) D_{\text{KL}}(\pi \parallel \pi_{\theta_k})[s] \leq \delta$, the KL divergence is convex w.r.t. its first argument, therefore constraint (14) which is a linear combination of convex

functions is also convex. Since π_{θ_k} satisfies Constraint (13) and is also an interior point within the set given by Constraints (14) ($D_{\text{KL}}(\pi_{\theta_k} \parallel \pi_{\theta_k}) = 0$, and $\delta > 0$), therefore Slater's constraint qualification holds, strong duality holds.

We can therefore solve for the optimal value of Problem (12-14) p^* by solving the corresponding dual problem. Let

$$L(\pi, \lambda, \nu) = \lambda \delta + \nu \tilde{b} + \mathbb{E}_{s \sim d^{\pi_{\theta_k}}} \left[\mathbb{E}_{a \sim \pi(\cdot|s)} [A^{\pi_{\theta_k}}(s, a)] - \nu \mathbb{E}_{a \sim \pi(\cdot|s)} [A_C^{\pi_{\theta_k}}(s, a)] - \lambda D_{\text{KL}}(\pi \parallel \pi_{\theta_k})[s] \right] \quad (18)$$

Therefore,

$$p^* = \max_{\pi \in \Pi} \min_{\lambda, \nu \geq 0} L(\pi, \lambda, \nu) = \min_{\lambda, \nu \geq 0} \max_{\pi \in \Pi} L(\pi, \lambda, \nu) \quad (19)$$

where we invoked strong duality in the second equality. We note that if π^*, λ^*, ν^* is optimal for (19), π^* is also optimal for Problem (12-14) (Boyd & Vandenberghe, 2004).

Consider the inner maximization problem in (19), we can decompose this problem into separate problems, one for each s . This gives us an optimization problem in the form of Problem (17), which is equivalent to the inner maximization problem in (19). By Lemma 1, the solution to (17) takes the form of (15). Plugging π^* back into Equation 19 gives us

$$\begin{aligned} p^* &= \min_{\lambda, \nu \geq 0} \lambda \delta + \nu \tilde{b} + \mathbb{E}_{\substack{s \sim d^{\pi_{\theta_k}} \\ a \sim \pi^*}} [A^{\pi_{\theta_k}}(s, a) - A_C^{\pi_{\theta_k}}(s, a) \\ &\quad - \lambda (\log \pi^*(a|s) - \log \pi_{\theta_k}(a|s))] \\ &= \min_{\lambda, \nu \geq 0} \lambda \delta + \nu \tilde{b} + \mathbb{E}_{\substack{s \sim d^{\pi_{\theta_k}} \\ a \sim \pi^*}} [A^{\pi_{\theta_k}}(s, a) - A_C^{\pi_{\theta_k}}(s, a) \\ &\quad - \lambda (\log \pi_{\theta_k}(a|s) - \log Z_{\lambda, \nu}(s)) \\ &\quad + \frac{1}{\lambda} (A^{\pi_{\theta_k}}(s, a) - \nu A_C^{\pi_{\theta_k}}(s, a) - \log \pi_{\theta_k}(a|s))] \\ &= \min_{\lambda, \nu \geq 0} \lambda \delta + \nu \tilde{b} + \lambda \mathbb{E}_{\substack{s \sim d^{\pi_{\theta_k}} \\ a \sim \pi^*}} [\log Z_{\lambda, \nu}(s)] \end{aligned}$$

□

The form of the optimal policy is intuitive, it gives high probability mass to areas of the state-action space with high return which is offset by the a penalty term times the cost advantage. We will refer to the optimal solution to (12-14) as the *optimal update policy*. We also note that it is possible to extend our results to accommodate for multiple constraints by introducing Lagrange multipliers $\nu_1, \dots, \nu_m \geq 0$, one for each cost constraint and applying a similar duality argument.

Another desirable property of the optimal update policy π^* is that for any feasible policy π_{θ_k} , it satisfies the following

bound for worst-case guarantee for cost constraint satisfaction from (Achiam et al., 2017):

$$J_C(\pi^*) \leq b + \frac{\sqrt{2\delta}\gamma\epsilon_C^{\pi^*}}{(1-\gamma)^2} \quad (20)$$

where $\epsilon_C^{\pi^*} = \max_s \left| \mathbb{E}_{a \sim \pi^*} [A_C^{\pi^*}(s, a)] \right|$.

3.2. Approximating the Optimal Update Policy

When solving Problem (12-14), we allow π to be in the set of all stationary policies Π thus the resulting π^* is no longer necessarily in the parameterized policy space Π_θ . Therefore in the second step we project the optimal update policy back into the parameterized policy space by minimizing the loss function:

$$\mathcal{L}(\theta) = \mathbb{E}_{s \sim d^{\pi^*}} [D_{\text{KL}}(\pi_\theta \| \pi^*) [s]] \quad (21)$$

Here $\pi_\theta \in \Pi_\theta$ is some projected policy which we will use to approximate the optimal update policy. We can use first-order methods to minimize this loss function where we will make use of the following result:

Corollary 1. *The gradient of $\mathcal{L}(\theta)$ takes the form*

$$\nabla_\theta \mathcal{L}(\theta) = \mathbb{E}_{s \sim d^{\pi^*}} [\nabla_\theta D_{\text{KL}}(\pi_\theta \| \pi^*) [s]] \quad (22)$$

where

$$\begin{aligned} \nabla_\theta D_{\text{KL}}(\pi_\theta \| \pi^*) [s] &= \nabla_\theta D_{\text{KL}}(\pi_\theta \| \pi_{\theta_k}) [s] \\ &- \frac{1}{\lambda} \mathbb{E}_{a \sim \pi_{\theta_k}} \left[\frac{\nabla_\theta \pi_\theta(a|s)}{\pi_{\theta_k}(a|s)} \left(A^{\pi_{\theta_k}}(s, a) - \nu A_C^{\pi_{\theta_k}}(s, a) \right) \right] \end{aligned} \quad (23)$$

Proof. See Appendix B in the supplementary materials. \square

Note that (22) can be estimated by sampling from the trajectories generated by policy π_{θ_k} which allows us to train our policy using stochastic gradients.

Corollary 1 provides an outline for our algorithm. At every iteration we begin with a policy π_{θ_k} , which we use to run trajectories and gather data. We use that data and (16) to first estimate λ and ν . We then draw a minibatch from the data to estimate $\nabla_\theta \mathcal{L}(\theta)$ given in Corollary 1. After taking a gradient step using Equation (22), we draw another minibatch and repeat the process.

3.3. Practical Implementation

Solving the dual problem (16) is computationally impractical for large state/action spaces as it requires calculating the partition function $Z_{\lambda, \nu}(s)$ which often involves evaluating a high-dimensional integral or sum. Furthermore, λ and ν depends on k and should be adapted at every iteration. In practice, a fixed λ found through hyperparameter sweeps

provides good results. However ν needs to be continuously adapted during training so as to ensure cost constraint satisfaction. Here we appeal to an intuitive heuristic for determining ν based on primal-dual gradient methods (Bertsekas, 2014). Recall that by strong duality, the optimal λ^* and ν^* minimizes $L(\pi^*, \lambda, \nu)$. We can therefore apply gradient descent w.r.t. ν to minimize $L(\pi^*, \lambda, \nu)$. We can show that

Corollary 2. *The derivative of $L(\pi^*, \lambda, \nu)$ w.r.t. ν is*

$$\frac{\partial L(\pi^*, \lambda, \nu)}{\partial \nu} = \tilde{b} - \mathbb{E}_{\substack{s \sim d^{\pi_{\theta_k}} \\ a \sim \pi^*}} [A^{\pi_{\theta_k}}(s, a)] \quad (24)$$

Proof. See Appendix C of the supplementary materials. \square

The last term in the gradient expression in Equation (24) cannot be evaluated since we do not have access to π^* . However since π_{θ_k} and π^* are 'close' (by constraint (14)), it is reasonable to assume that $E_{s \sim d^{\pi_{\theta_k}}, a \sim \pi^*} [A^{\pi_{\theta_k}}(s, a)] \approx E_{s \sim d^{\pi_{\theta_k}}, a \sim \pi_{\theta_k}} [A^{\pi_{\theta_k}}(s, a)] = 0$. In practice we find that this term can be set to zero which gives the update term:

$$\nu \leftarrow \underset{\nu}{\text{proj}} [\nu - \alpha(b - J_C(\pi_{\theta_k}))] \quad (25)$$

where α is the step size, here we have incorporated the discount term $(1 - \gamma)$ in \tilde{b} into the step size. The projection operator proj_ν projects ν back into the interval $[0, \nu_{\text{max}}]$ where ν_{max} is chosen so that ν does not become too large. However we will show in later sections that FOCOPS is generally insensitive to the choice of ν_{max} and setting $\nu_{\text{max}} = +\infty$ does not appear to greatly reduce performance. Practically, $J_C(\pi_{\theta_k})$ can be estimated via Monte Carlo methods using trajectories collected from π_{θ_k} . We note that the update rule in Equation (25) is similar in to the update rule introduced in (Chow et al., 2017). We recall that in (15), ν acts as a cost penalty term where increasing ν makes it less likely for state-action pairs with higher costs to be sampled by π^* . Hence in this regard, the update rule in (25) is intuitive in that it increases ν if $J_C(\pi_{\theta_k}) > b$ (i.e. the cost constraint is violated for π_{θ_k}) and decreases ν otherwise. Using the update rule (25), we can then perform one update step on ν before updating the policy parameters θ .

In order to mitigate the effects of sampling errors to better guarantee trust region constraint satisfaction we also add to (22) a per-state acceptance indicator function $I(s_j) := \mathbf{1}_{D_{\text{KL}}(\pi_\theta \| \pi_{\theta_k})[s_j] \leq \delta}$. This way sampled states whose $D_{\text{KL}}(\pi_\theta \| \pi_{\theta_k}) [s]$ is too large are rejected from the gradient update. The resulting sample gradient update term is

$$\begin{aligned} \hat{\nabla}_\theta \mathcal{L}(\theta) &\approx \frac{1}{N} \sum_{j=1}^N \left[\nabla_\theta D_{\text{KL}}(\pi_\theta \| \pi_{\theta_k}) [s_j] \right. \\ &\left. - \frac{1}{\lambda} \frac{\nabla_\theta \pi_\theta(a_j|s_j)}{\pi_{\theta_k}(a_j|s_j)} \left(\hat{A}(s_j, a_j) - \nu \hat{A}_C(s_j, a_j) \right) \right] I(s_j). \end{aligned} \quad (26)$$

Algorithm 1 FOCOPS Outline

Input: Policy network π_{θ_0} , Value networks $V_{\phi_0}, V_{\psi_0}^C$.

repeat

 Generate trajectories $\tau \sim \pi_{\theta_k}$.

 Estimate C -returns and advantage functions.

 Update ν using Equation (25).

for K epochs **do**

for each minibatch **do**

 Update value networks by minimizing MSE of $V_{\phi_k}, V_{\phi_k}^{\text{target}}$ and $V_{\psi_k}^C, V_{\psi_k}^{C,\text{target}}$.

 Update policy network using Equation (26)

end for

if $\frac{1}{N} \sum_{j=1}^N D_{\text{KL}}(\pi_{\theta} \parallel \pi_{\theta_k}) [s_j] > \delta$ **then**

 Break out of inner loop

end if

end for

until stopping criteria met

Here N is the number of samples we collected using policy π_{θ_k} , \hat{A} and \hat{A}_C are estimates of the advantage functions (for the return and cost) obtained from critic networks. We estimate the advantage functions using the Generalized Advantage Estimator (GAE) (Schulman et al., 2015b). We can then apply stochastic gradient descent using Equation (26). During training, we use the early stopping criteria $\frac{1}{N} \sum_{i=1}^N D_{\text{KL}}(\pi_{\theta} \parallel \pi_{\theta_k}) [s_i] > \delta$ which helps prevent trust region constraint violation for the new updated policy. We update the parameters for the value net by minimizing the Mean Square Error (MSE) of the value net output and some target value (which can be estimated via Monte Carlo or bootstrap estimates of the return).

We emphasize again that FOCOPS only requires first order methods (gradient descent) and is thus extremely simple to implement. Algorithm 1 presents a summary of the FOCOPS algorithm. A more detailed description of the algorithm is provided in Appendix D of the supplementary materials.

4. Experiments

We designed two different sets of experiments to test the efficacy of the FOCOPS algorithm. In the first set of experiments, we train different robotic agents to move along a straight line or a two dimensional plane, but the speed of the robot is constrained for safety purposes. The second set of experiments is inspired by the Circle experiments from (Achiam et al., 2017). Both sets of experiments are implemented using the OpenAI Gym API (Brockman et al., 2016) for the MuJoCo physical simulator (Todorov et al., 2012).

In addition to the CPO algorithm, we are also including for comparison two algorithms based on Lagrangian methods

(Bertsekas, 1997), which uses adaptive penalty coefficients to enforce constraints. For an objective function $f(\theta)$ and constraint $g(\theta) \leq 0$, the Lagrangian method solves max-min optimization problem $\max_{\theta} \min_{\nu \geq 0} (f(\theta) - \nu g(\theta))$. These methods first perform gradient ascent on θ , and then gradient descent on ν . Chow et al. (2019) and Ray et al. (2019) combined Lagrangian method with PPO (Schulman et al., 2017) and TRPO to form the PPO Lagrangian and TRPO Lagrangian algorithms, which we will subsequently abbreviate as PPO-L and TRPO-L respectively.

4.1. Robots with Speed Limit

We consider six MuJoCo environments where we attempt to train a robotic agent to move along a one-dimensional line or on a two-dimensional plane (see Appendix E.1 of the supplementary material for details). However we impose a speed limit on our environments. The goal is then to obtain the maximum possible return while keeping the agent’s speed under some threshold. The cost thresholds are calculated using 50% of the speed attained by an unconstrained PPO agent after training for a million samples.

Figure 1 shows the learning curves for the robots with speed limit tasks averaged over 10 random seeds where we plotted the bootstrap mean and normal 95% confidence interval of 1000 bootstrap samples (Efron & Tibshirani, 1994). As recommended by Henderson et al. (2018), we used the bootstrap approach to gain more insight into our results due to the small sample size (10 random seeds). An unconstrained PPO agent is also plotted for comparison. On all tasks, FOCOPS is able to consistently enforce approximate constraint satisfaction while having a higher performance on five out of the six tasks. The performance difference is even more notable on some of the more challenging tasks such as Humanoid. We also note that Lagrangian methods outperform CPO on several environments; this however is achieved at the cost of poor constraint satisfaction (most notably in the HalfCheetah and Hopper environments).

In Table 1 we summarized the results of all four algorithms using a normalized value of the reward/cost return, which is calculated as a percentage of the average return for reward/cost of an unconstrained PPO agent after training for the same number of samples (e.g. for Ant-v3, after training PPO-Lagrangian for 1 million samples, the agent obtained 70.5% of the return and 49.0% of the cost of an unconstrained PPO agent). The bootstrap normal 95% bootstrap confidence interval is also included.

4.2. Circle Tasks

For these tasks, we use the same exact geometric setting, reward, and cost constraint function as (Achiam et al., 2017), a geometric illustration of the task and details on the reward/cost functions can be found in Appendix E.2 of the

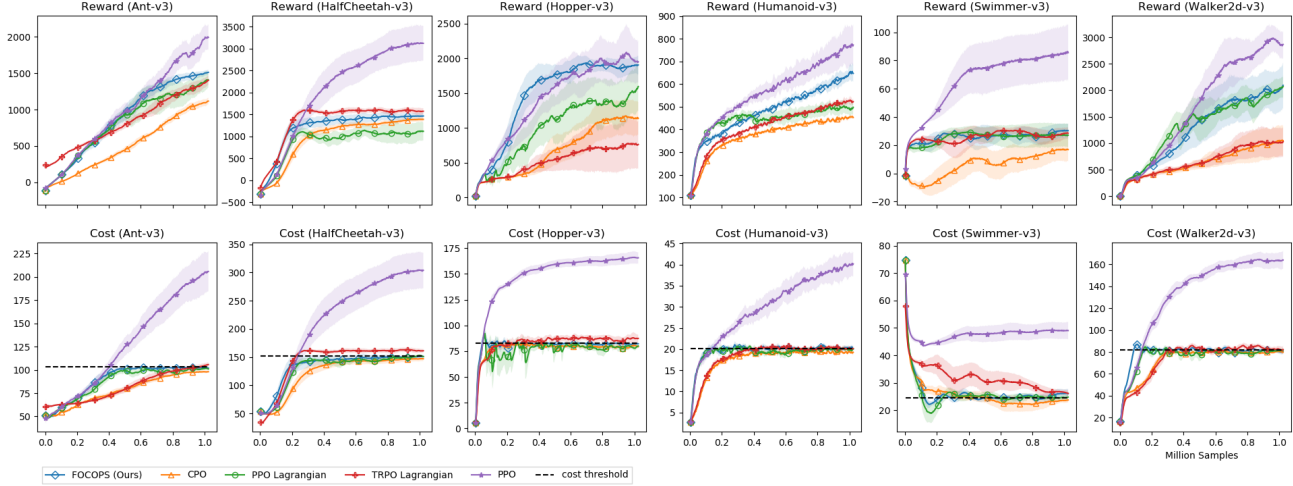


Figure 1. Comparing reward and cost returns for six robots with speed limit tasks. The x -axis represent the number of samples used and the y -axis represent the average total reward/cost return of the last 100 episodes. The solid line represent the mean of 1000 bootstrap samples over 10 random seeds. The shaded regions represent the bootstrap normal 95% confidence interval.

supplementary materials. The goal of the agents is to move along the circumference of a circle while remaining within a safe region smaller than the radius of the circle.

Similar to the previous tasks, we provide learning curves (Figure 2) and (normalized) numerical summaries (Table 2) of the experiments. On these tasks, all four approaches are able to approximately enforce cost constraint satisfaction, but FOCOPS does so while having a higher performance. Note for both tasks, the 95% confidence interval for FOCOPS lies above the confidence intervals for all other algorithms (excluding the unconstrained PPO agent), this is strong indication that FOCOPS outperforms the other three algorithms on these particular tasks.

4.3. Generalization Analysis

In supervised learning, the standard approach is to use separate datasets for training, validation, and testing where we can then use some evaluation metric on the test set to determine how well an algorithm generalizes over unseen data. However such a scheme can be challenging and often impractical to implement in reinforcement learning.

To similarly evaluate our reinforcement learning agent, we first trained our agent on a fixed random seed. We then test the trained agent on ten unseen random seeds. This approach was proposed by Joelle Pineau (2018). The average (reward) return over the ten unseen seeds averaged across all environments are reported in Table 3. We find that FOCOPS is able to outperform the other three algorithms on unseen random seeds while maintaining approximate constraint satisfaction. Detailed analysis of the generalization results are

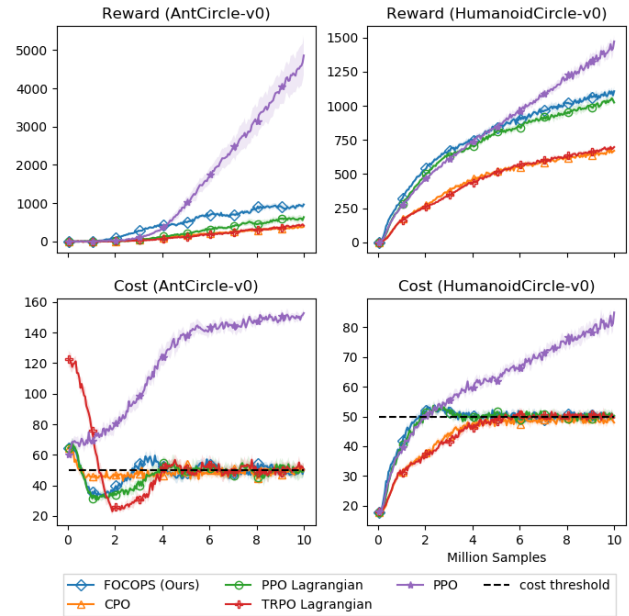


Figure 2. Comparing reward and cost returns on circle Tasks. The x -axis represent the number of samples used and the y -axis represent the average total reward/cost return of the last 100 episodes. The solid line represent the mean of 1000 bootstrap samples over 10 random seeds. The shaded regions represent the bootstrap normal 95% confidence interval.

Table 1. Bootstrap mean and normal 95% confidence interval with 1000 bootstrap samples over 10 random seeds of (normalized) reward/cost return after training on robot with speed limit environments for 1 million samples.

Environment		PPO-L	TRPO-L	CPO	FOCOPS
Ant-v3	Reward	0.705 ± 0.056	0.700 ± 0.033	0.558 ± 0.022	0.755 ± 0.017
	Cost	0.490 ± 0.006	0.513 ± 0.011	0.476 ± 0.004	0.495 ± 0.004
HalfCheetah-v3	Reward	0.356 ± 0.066	0.503 ± 0.023	0.444 ± 0.015	0.468 ± 0.021
	Cost	0.496 ± 0.005	0.529 ± 0.011	0.483 ± 0.012	0.497 ± 0.007
Hopper-v3	Reward	0.808 ± 0.173	0.389 ± 0.173	0.576 ± 0.120	0.972 ± 0.067
	Cost	0.484 ± 0.011	0.528 ± 0.022	0.480 ± 0.006	0.492 ± 0.011
Humanoid-v3	Reward	0.649 ± 0.036	0.681 ± 0.015	0.590 ± 0.008	0.844 ± 0.048
	Cost	0.498 ± 0.013	0.499 ± 0.01	0.478 ± 0.012	0.499 ± 0.015
Swimmer-v3	Reward	0.314 ± 0.100	0.336 ± 0.047	0.199 ± 0.100	0.352 ± 0.057
	Cost	0.504 ± 0.020	0.533 ± 0.021	0.483 ± 0.020	0.495 ± 0.035
Walker2d-v3	Reward	0.721 ± 0.069	0.360 ± 0.097	0.365 ± 0.097	0.727 ± 0.136
	Cost	0.498 ± 0.013	0.502 ± 0.020	0.487 ± 0.035	0.488 ± 0.013

Table 2. Bootstrap mean and normal 95% confidence interval with 1000 bootstrap samples over 10 random seeds of (normalized) reward/cost return after training on circle environments for 10 million samples.

Environment		PPO-L	TRPO-L	CPO	FOCOPS
Ant-Circle	Reward	0.131 ± 0.019	0.086 ± 0.009	0.08 ± 0.009	0.199 ± 0.010
	Cost	0.330 ± 0.029	0.330 ± 0.029	0.327 ± 0.023	0.326 ± 0.014
Humanoid-Circle	Reward	0.695 ± 0.016	0.473 ± 0.010	0.455 ± 0.009	0.751 ± 0.022
	Cost	0.592 ± 0.007	0.584 ± 0.011	0.564 ± 0.017	0.587 ± 0.010

provided in Appendix E.3 of the supplementary materials.

Table 3. Mean (normalized) return of 10 episodes for pretrained PPO Lagrangian, TRPO Lagrangian, CPO, and FOCOPS agents on 10 unseen random seeds averaged across all environments.

	PPO-L	TRPO-L	CPO	FOCOPS
Speed Limit	0.718	0.604	0.747	0.860
Circle	0.262	0.169	0.157	0.277

4.4. Sensitivity Analysis

FOCOPS introduces two additional hyperparameters λ and ν_{\max} . However we find that the performance of FOCOPS is largely insensitive to the choice of these hyperparameters. To demonstrate this, we conducted a series of experiments on the robots with speed limit tasks.

For FOCOPS, PPO Lagrangian, and TRPO Lagrangian, the hyperparameter ν_{\max} was selected via hyperparameter sweep on the set $\{1, 2, 3, 5, 10, +\infty\}$ where the best per-

forming hyperparameter for each algorithm which approximately enforces the cost constraint was chosen. However we found that FOCOPS is not sensitive to the choice of ν_{\max} where setting $\nu_{\max} = +\infty$ only leads to an average 0.3% degradation in performance compared to the optimal $\nu_{\max} = 2$. Similarly we tested the performance of FOCOPS against different values of λ where in the worst case FOCOPS performs on average 2.3% worse compared to the optimal $\lambda = 1.3$. See Appendix E.4 of the supplementary materials for more details.

5. Conclusion

In this paper, we introduced the FOCOPS methodology, which uses a principled two-step approach to solve the constrained reinforcement learning problem. Our approach is first order in nature thus easy to implement and enjoys an approximate feasibility guarantee during training. We have shown that the FOCOPS algorithm is able to train on large neural network policies and outperforms second-order algorithms such as CPO and other approaches on high-dimensional constrained robotics control tasks.

6. Acknowledgement

The authors would like to express our appreciation for the technical support provided by the NYU Shanghai High Performance Computing (HPC) administrator Zhiguo Qi and the HPC team at NYU. We would also like to thank Joshua Achiam for his insightful comments and for making his implementation of the CPO algorithm publicly available.

References

- Achiam, J., Held, D., Tamar, A., and Abbeel, P. Constrained policy optimization. In *Proceedings of the 34th International Conference on Machine Learning-Volume 70*, pp. 22–31. JMLR. org, 2017.
- Altman, E. *Constrained Markov decision processes*, volume 7. CRC Press, 1999.
- Amodei, D., Olah, C., Steinhardt, J., Christiano, P., Schulman, J., and Mané, D. Concrete problems in ai safety. *arXiv preprint arXiv:1606.06565*, 2016.
- Bertsekas, D. P. Nonlinear programming. *Journal of the Operational Research Society*, 48(3):334–334, 1997.
- Bertsekas, D. P. *Constrained optimization and Lagrange multiplier methods*. Academic press, 2014.
- Beutler, F. J. and Ross, K. W. Optimal policies for controlled markov chains with a constraint. *Journal of mathematical analysis and applications*, 112(1):236–252, 1985.
- Beutler, F. J. and Ross, K. W. Time-average optimal constrained semi-markov decision processes. *Advances in Applied Probability*, 18(2):341–359, 1986.
- Boyd, S. and Vandenberghe, L. *Convex optimization*. Cambridge university press, 2004.
- Brockman, G., Cheung, V., Pettersson, L., Schneider, J., Schulman, J., Tang, J., and Zaremba, W. Openai gym, 2016.
- Chow, Y., Ghavamzadeh, M., Janson, L., and Pavone, M. Risk-constrained reinforcement learning with percentile risk criteria. *The Journal of Machine Learning Research*, 18(1):6070–6120, 2017.
- Chow, Y., Nachum, O., Faust, A., Ghavamzadeh, M., and Duenez-Guzman, E. Lyapunov-based safe policy optimization for continuous control. *arXiv preprint arXiv:1901.10031*, 2019.
- Duan, Y., Chen, X., Houthoofd, R., Schulman, J., and Abbeel, P. Benchmarking deep reinforcement learning for continuous control. In *International Conference on Machine Learning*, pp. 1329–1338, 2016.
- Efron, B. and Tibshirani, R. J. *An introduction to the bootstrap*. CRC press, 1994.
- Haarnoja, T., Zhou, A., Abbeel, P., and Levine, S. Soft actor-critic: Off-policy maximum entropy deep reinforcement learning with a stochastic actor. *International Conference on Machine Learning (ICML)*, 2018.
- Henderson, P., Islam, R., Bachman, P., Pineau, J., Precup, D., and Meger, D. Deep reinforcement learning that matters. In *Thirty-Second AAAI Conference on Artificial Intelligence*, 2018.
- Kakade, S. and Langford, J. Approximately optimal approximate reinforcement learning. In *International Conference on Machine Learning*, volume 2, pp. 267–274, 2002.
- Kallenberg, L. *Linear Programming and Finite Markovian Control Problems*. Centrum Voor Wiskunde en Informatica, 1983.
- Mnih, V., Kavukcuoglu, K., Silver, D., Graves, A., Antonoglou, I., Wierstra, D., and Riedmiller, M. Playing atari with deep reinforcement learning. *arXiv preprint arXiv:1312.5602*, 2013.
- Mnih, V., Badia, A. P., Mirza, M., Graves, A., Lillicrap, T., Harley, T., Silver, D., and Kavukcuoglu, K. Asynchronous methods for deep reinforcement learning. In *International Conference on Machine Learning (ICML)*, pp. 1928–1937, 2016.
- Peters, J. and Schaal, S. Reinforcement learning of motor skills with policy gradients. *Neural networks*, 21(4):682–697, 2008.
- Pineau, J. Reproducible, reusable, and robust reinforcement learning, 2018.
- Pirotta, M., Restelli, M., Pecorino, A., and Calandriello, D. Safe policy iteration. In *International Conference on Machine Learning*, pp. 307–315, 2013.
- Ray, A., Achiam, J., and Amodei, D. Benchmarking Safe Exploration in Deep Reinforcement Learning. 2019.
- Ross, K. W. Constrained markov decision processes with queueing applications. *Dissertation Abstracts International Part B: Science and Engineering[DISS. ABST. INT. PT. B- SCI. & ENG.]*, 46(4), 1985.
- Ross, K. W. Randomized and past-dependent policies for markov decision processes with multiple constraints. *Operations Research*, 37(3):474–477, 1989.
- Ross, K. W. and Varadarajan, R. Markov decision processes with sample path constraints: the communicating case. *Operations Research*, 37(5):780–790, 1989.

- Ross, K. W. and Varadarajan, R. Multichain markov decision processes with a sample path constraint: A decomposition approach. *Mathematics of Operations Research*, 16(1):195–207, 1991.
- Schaul, T., Quan, J., Antonoglou, I., and Silver, D. Prioritized experience replay. *arXiv preprint arXiv:1511.05952*, 2015.
- Schulman, J., Levine, S., Abbeel, P., Jordan, M., and Moritz, P. Trust region policy optimization. In *International Conference on Machine Learning*, pp. 1889–1897, 2015a.
- Schulman, J., Moritz, P., Levine, S., Jordan, M., and Abbeel, P. High-dimensional continuous control using generalized advantage estimation. *arXiv preprint arXiv:1506.02438*, 2015b.
- Schulman, J., Wolski, F., Dhariwal, P., Radford, A., and Klimov, O. Proximal policy optimization algorithms. *arXiv preprint arXiv:1707.06347*, 2017.
- Silver, D., Huang, A., Maddison, C. J., Guez, A., Sifre, L., Van Den Driessche, G., Schrittwieser, J., Antonoglou, I., Panneershelvam, V., Lanctot, M., et al. Mastering the game of go with deep neural networks and tree search. *nature*, 529(7587):484, 2016.
- Silver, D., Hubert, T., Schrittwieser, J., Antonoglou, I., Lai, M., Guez, A., Lanctot, M., Sifre, L., Kumaran, D., Graepel, T., et al. Mastering chess and shogi by self-play with a general reinforcement learning algorithm. *arXiv preprint arXiv:1712.01815*, 2017.
- Strang, G. *Computational science and engineering*. Wellesley-Cambridge Press, 2007.
- Sutton, R. S. and Barto, A. G. *Reinforcement learning: An introduction*. MIT press, 2018.
- Tessler, C., Mankowitz, D. J., and Mannor, S. Reward constrained policy optimization. *arXiv preprint arXiv:1805.11074*, 2018.
- Todorov, E., Erez, T., and Tassa, Y. Mujoco: A physics engine for model-based control. In *2012 IEEE/RSJ International Conference on Intelligent Robots and Systems*, pp. 5026–5033. IEEE, 2012.
- Van Hasselt, H., Guez, A., and Silver, D. Deep reinforcement learning with double q-learning. In *AAAI*, volume 2, pp. 5. Phoenix, AZ, 2016.
- Vuong, Q., Zhang, Y., and Ross, K. W. Supervised policy update for deep reinforcement learning. In *International Conference on Learning Representation*, 2019.
- Wang, Z., Bapst, V., Heess, N., Mnih, V., Munos, R., Kavukcuoglu, K., and de Freitas, N. Sample efficient actor-critic with experience replay. *International Conference on Learning Representations (ICLR)*, 2017.
- Wu, Y., Mansimov, E., Grosse, R. B., Liao, S., and Ba, J. Scalable trust-region method for deep reinforcement learning using kronecker-factored approximation. In *Advances in neural information processing systems (NIPS)*, pp. 5285–5294, 2017.
- Yang, T.-Y., Rosca, J., Narasimhan, K., and Ramadge, P. J. Projection-based constrained policy optimization. In *International Conference on Learning Representation*, 2020.

First Order Optimization in Policy Space for Constrained Deep Reinforcement Learning

Supplementary Materials

Appendices

A. Proof of Lemma 1

Lemma 1. For fixed s , $\lambda > 0$, and $\nu \geq 0$, the solution to the optimization problem:

$$\begin{aligned}
 & \underset{\pi}{\text{maximize}} && \mathbb{E}_{a \sim \pi(\cdot|s)} \left[A^{\pi_{\theta_k}}(s, a) - \nu A_C^{\pi_{\theta_k}}(s, a) \right. \\
 & && \left. - \lambda (\log \pi(a|s) - \log \pi_{\theta_k}(a|s)) \right] \\
 & \text{subject to} && \sum_a \pi(a|s) = 1 \\
 & && \pi(a|s) \geq 0 \quad \text{for all } a \in \mathcal{A}
 \end{aligned} \tag{17}$$

is given by (15).

Proof. First observe that this problem is convex (maximizing a concave objective subject to a linear constraint). Since the problem only consists of one linear equality, Slater's constraint qualifications, and hence strong duality holds. We can therefore solve this problem via the corresponding dual problem (Boyd & Vandenberghe, 2004).

We can write the Lagrangian of (17) as

$$\begin{aligned}
 G(\pi) = & \sum_a \pi(a|s) \left[A^{\pi_{\theta_k}}(s, a) - \nu A_C^{\pi_{\theta_k}}(s, a) \right. \\
 & \left. - \lambda (\log \pi(a|s) - \log \pi_{\theta_k}(a|s)) + \zeta \right] - 1
 \end{aligned} \tag{27}$$

where $\zeta > 0$ is the Lagrange multiplier associated with the constraint $\sum_a \pi(a|s) = 1$. Differentiating $G(\pi)$ w.r.t. $\pi(a|s)$ for some a :

$$\begin{aligned}
 \frac{\partial G}{\partial \pi(a|s)} = & A^{\pi_{\theta_k}}(s, a) - \nu A_C^{\pi_{\theta_k}}(s, a) \\
 & - \lambda (\log \pi(a|s) + 1 - \log \pi_{\theta_k}(a|s)) + \zeta
 \end{aligned} \tag{28}$$

Setting (28) to zero and rearranging the term, we obtain

$$\pi(a|s) = \pi_{\theta_k}(a|s) \exp \left(\frac{1}{\lambda} \left(A^{\pi_{\theta_k}}(s, a) - \nu A_C^{\pi_{\theta_k}}(s, a) \right) + \frac{\zeta}{\lambda} + 1 \right) \tag{29}$$

We chose ζ so that $\sum_a \pi(a|s) = 1$ and rewrite $\zeta/\lambda + 1$ as $Z_{\lambda, \nu}(s)$. We find that the optimal solution to (17) takes the form (15). \square

B. Proof of Corollary 1

Corollary 1. The gradient of $\mathcal{L}(\theta)$ takes the form

$$\nabla_{\theta} \mathcal{L}(\theta) = \mathbb{E}_{s \sim d^{\pi_{\theta_k}}} [\nabla_{\theta} D_{KL}(\pi_{\theta} \| \pi^*) [s]] \tag{22}$$

where

$$\begin{aligned} \nabla_{\theta} D_{\text{KL}}(\pi_{\theta} \|\pi^{*})[s] &= \nabla_{\theta} D_{\text{KL}}(\pi_{\theta} \|\pi_{\theta_k})[s] \\ &- \frac{1}{\lambda} \mathbb{E}_{a \sim \pi_{\theta_k}} \left[\frac{\nabla_{\theta} \pi_{\theta}(a|s)}{\pi_{\theta_k}(a|s)} \left(A^{\pi_{\theta_k}}(s, a) - \nu A_C^{\pi_{\theta_k}}(s, a) \right) \right] \end{aligned} \quad (23)$$

Proof. We only need to calculate the gradient of the loss function for a single sampled s . We first note that,

$$\begin{aligned} D_{\text{KL}}(\pi_{\theta} \|\pi^{*})[s] &= - \sum_a \pi_{\theta}(a|s) \log \pi^{*}(a|s) + \sum_a \pi_{\theta}(a|s) \log \pi_{\theta}(a|s) \\ &= H(\pi_{\theta}, \pi^{*})[s] - H(\pi_{\theta})[s] \end{aligned}$$

where $H(\pi_{\theta})[s]$ is the entropy and $H(\pi_{\theta}, \pi^{*})[s]$ is the cross-entropy under state s . We expand the cross entropy term which gives us

$$\begin{aligned} H(\pi_{\theta}, \pi^{*})[s] &= - \sum_a \pi_{\theta}(a|s) \log \pi^{*}(a|s) \\ &= - \sum_a \pi_{\theta}(a|s) \log \left(\frac{\pi_{\theta_k}(a|s)}{Z_{\lambda, \nu}(s)} \exp \left[\frac{1}{\lambda} \left(A^{\pi_{\theta_k}}(s, a) - \nu A_C^{\pi_{\theta_k}}(s, a) \right) \right] \right) \\ &= - \sum_a \pi_{\theta}(a|s) \log \pi_{\theta_k}(a|s) + \log Z_{\lambda, \nu}(s) - \frac{1}{\lambda} \sum_a \pi_{\theta}(a|s) \left(A^{\pi_{\theta_k}}(s, a) - \nu A_C^{\pi_{\theta_k}}(s, a) \right) \end{aligned}$$

We then subtract the entropy term to recover the KL divergence:

$$\begin{aligned} D_{\text{KL}}(\pi_{\theta} \|\pi^{*})[s] &= D_{\text{KL}}(\pi_{\theta} \|\pi_{\theta_k})[s] + \log Z_{\lambda, \nu}(s) - \frac{1}{\lambda} \sum_a \pi_{\theta}(a|s) \left(A^{\pi_{\theta_k}}(s, a) - \nu A_C^{\pi_{\theta_k}}(s, a) \right) \\ &= D_{\text{KL}}(\pi_{\theta} \|\pi_{\theta_k})[s] + \log Z_{\lambda, \nu}(s) - \frac{1}{\lambda} \mathbb{E}_{a \sim \pi_{\theta_k}(\cdot|s)} \left[\frac{\pi_{\theta}(a|s)}{\pi_{\theta_k}(a|s)} \left(A^{\pi_{\theta_k}}(s, a) - \nu A_C^{\pi_{\theta_k}}(s, a) \right) \right] \end{aligned}$$

where in the last equality we applied importance sampling to rewrite the expectation w.r.t. π_{θ_k} . Finally, taking the gradient on both sides gives us:

$$\nabla_{\theta} D_{\text{KL}}(\pi_{\theta} \|\pi^{*})[s] = \nabla_{\theta} D_{\text{KL}}(\pi_{\theta} \|\pi_{\theta_k})[s] - \frac{1}{\lambda} \mathbb{E}_{a \sim \pi_{\theta_k}(\cdot|s)} \left[\frac{\nabla_{\theta} \pi_{\theta}(a|s)}{\pi_{\theta_k}(a|s)} \left(A^{\pi_{\theta_k}}(s, a) - \nu A_C^{\pi_{\theta_k}}(s, a) \right) \right].$$

□

C. Proof of Corollary 2

Corollary 2. *The derivative of $L(\pi^{*}, \lambda, \nu)$ w.r.t. ν is*

$$\frac{\partial L(\pi^{*}, \lambda, \nu)}{\partial \nu} = \tilde{b} - \mathbb{E}_{\substack{s \sim d^{\pi_{\theta_k}} \\ a \sim \pi^{*}}} [A^{\pi_{\theta_k}}(s, a)] \quad (24)$$

Proof. From Theorem 1, we have

$$L(\pi^{*}, \lambda, \nu) = \lambda \delta + \nu \tilde{b} + \lambda \mathbb{E}_{\substack{s \sim d^{\pi_{\theta_k}} \\ a \sim \pi^{*}}} [\log Z_{\lambda, \nu}(s)]. \quad (30)$$

The first two terms is an affine function w.r.t. ν , therefore its derivative is \tilde{b} . We will then focus on the expectation in the last term. To simplify our derivation, we will first calculate the derivative of π^{*} w.r.t. ν ,

$$\begin{aligned} \frac{\partial \pi^{*}(a|s)}{\partial \nu} &= \frac{\pi_{\theta_k}(a|s)}{Z_{\lambda, \nu}^2(s)} \left[Z_{\lambda, \nu}(s) \frac{\partial}{\partial \nu} \exp \left(\frac{1}{\lambda} \left(A^{\pi_{\theta_k}}(s, a) - \nu A_C^{\pi_{\theta_k}}(s, a) \right) \right) - \exp \left(\frac{1}{\lambda} \left(A^{\pi_{\theta_k}}(s, a) - \nu A_C^{\pi_{\theta_k}}(s, a) \right) \right) \frac{\partial Z_{\lambda, \nu}(s)}{\partial \nu} \right] \\ &= - \frac{A_C^{\pi_{\theta_k}}(s, a)}{\lambda} \pi^{*}(a|s) - \pi^{*}(a|s) \frac{\partial \log Z_{\lambda, \nu}(s)}{\partial \nu} \end{aligned}$$

Therefore the derivative of the expectation in the last term of $L(\pi^*, \lambda, \nu)$ can be written as

$$\begin{aligned}
 \frac{\partial}{\partial \nu} \mathbb{E}_{\substack{s \sim d^{\pi_{\theta_k}} \\ a \sim \pi^*}} [\log Z_{\lambda, \nu}(s)] &= \mathbb{E}_{\substack{s \sim d^{\pi_{\theta_k}} \\ a \sim \pi_{\theta_k}}} \left[\frac{\partial}{\partial \nu} \left(\frac{\pi^*(a|s)}{\pi_{\theta_k}(a|s)} \log Z_{\lambda, \nu}(s) \right) \right] \\
 &= \mathbb{E}_{\substack{s \sim d^{\pi_{\theta_k}} \\ a \sim \pi_{\theta_k}}} \left[\frac{1}{\pi_{\theta_k}(a|s)} \left(\frac{\partial \pi^*(a|s)}{\partial \nu} \log Z_{\lambda, \nu}(s) + \pi^*(a|s) \frac{\partial \log Z_{\lambda, \nu}(s)}{\partial \nu} \right) \right] \\
 &= \mathbb{E}_{\substack{s \sim d^{\pi_{\theta_k}} \\ a \sim \pi_{\theta_k}}} \left[\frac{\pi^*(a|s)}{\pi_{\theta_k}(a|s)} \left(-\frac{A_C^{\pi_{\theta_k}}(s, a)}{\lambda} \log Z_{\lambda, \nu}(s) - \frac{\partial \log Z_{\lambda, \nu}(s)}{\partial \nu} \log Z_{\lambda, \nu}(s) + \frac{\partial \log Z_{\lambda, \nu}(s)}{\partial \nu} \right) \right] \\
 &= \mathbb{E}_{\substack{s \sim d^{\pi_{\theta_k}} \\ a \sim \pi^*}} \left[-\frac{A_C^{\pi_{\theta_k}}(s, a)}{\lambda} \log Z_{\lambda, \nu}(s) - \frac{\partial \log Z_{\lambda, \nu}(s)}{\partial \nu} \log Z_{\lambda, \nu}(s) + \frac{\partial \log Z_{\lambda, \nu}(s)}{\partial \nu} \right].
 \end{aligned} \tag{31}$$

Also,

$$\begin{aligned}
 \frac{\partial Z_{\lambda, \nu}(s)}{\partial \nu} &= \frac{\partial}{\partial \nu} \sum_a \pi_{\theta_k}(a|s) \exp \left(\frac{1}{\lambda} \left(A^{\pi_{\theta_k}}(s, a) - \nu A_C^{\pi_{\theta_k}}(s, a) \right) \right) \\
 &= \sum_a -\pi_{\theta_k}(a|s) \frac{A_C^{\pi_{\theta_k}}(s, a)}{\lambda} \exp \left(\frac{1}{\lambda} \left(A^{\pi_{\theta_k}}(s, a) - \nu A_C^{\pi_{\theta_k}}(s, a) \right) \right) \\
 &= \sum_a -\frac{A_C^{\pi_{\theta_k}}(s, a)}{\lambda} \frac{\pi_{\theta_k}(a|s)}{Z_{\lambda, \nu}(s)} \exp \left(\frac{1}{\lambda} \left(A^{\pi_{\theta_k}}(s, a) - \nu A_C^{\pi_{\theta_k}}(s, a) \right) \right) Z_{\lambda, \nu}(s) \\
 &= -\frac{Z_{\lambda, \nu}(s)}{\lambda} \mathbb{E}_{a \sim \pi^*(\cdot|s)} \left[A_C^{\pi_{\theta_k}}(s, a) \right].
 \end{aligned} \tag{32}$$

Therefore,

$$\frac{\partial \log Z_{\lambda, \nu}(s)}{\partial \nu} = \frac{\partial Z_{\lambda, \nu}(s)}{\partial \nu} \frac{1}{Z_{\lambda, \nu}(s)} = -\frac{1}{\lambda} \mathbb{E}_{a \sim \pi^*(\cdot|s)} \left[A_C^{\pi_{\theta_k}}(s, a) \right]. \tag{33}$$

Plugging (33) into the last equality in (31) gives us

$$\begin{aligned}
 \frac{\partial}{\partial \nu} \mathbb{E}_{\substack{s \sim d^{\pi_{\theta_k}} \\ a \sim \pi^*}} [\log Z_{\lambda, \nu}(s)] &= \mathbb{E}_{\substack{s \sim d^{\pi_{\theta_k}} \\ a \sim \pi^*}} \left[-\frac{A_C^{\pi_{\theta_k}}(s, a)}{\lambda} \log Z_{\lambda, \nu}(s) + \frac{A_C^{\pi_{\theta_k}}(s, a)}{\lambda} \log Z_{\lambda, \nu}(s) - \frac{1}{\lambda} A_C^{\pi_{\theta_k}}(s, a) \right] \\
 &= -\frac{1}{\lambda} \mathbb{E}_{\substack{s \sim d^{\pi_{\theta_k}} \\ a \sim \pi^*}} \left[A_C^{\pi_{\theta_k}}(s, a) \right].
 \end{aligned} \tag{34}$$

Combining (34) with the derivatives of the affine term gives us the final desired result. \square

D. Pseudocode

Algorithm 2 First Order Constrained Optimization in Policy Space (FOCOPS)

Input: Policy network π_θ ; Value network for return V_ϕ ; Value network for costs V_ψ^C .

Input: Discount rates γ , GAE parameter β ; Learning rates $\alpha_\nu, \alpha_V, \alpha_\pi$; Temperature λ ; Initial cost constraint parameter ν ; Cost constraint parameter bound ν_{\max} . Trust region bound δ ; Per-state KL bound η ; Cost bound b .

repeat

Generate batch data of M episodes of length T from $(s_{i,t}, a_{i,t}, r_{i,t}, s_{i,t+1}, c_{i,t})$ from $\pi_\theta, i = 1, \dots, M, t = 1, \dots, T$.
Estimate C -return by averaging over C -return for all episodes:

$$\hat{J}_C = \frac{1}{M} \sum_{i=1}^M \sum_{t=0}^{T-1} \gamma^t c_{i,t}$$

Store old policy $\theta' \leftarrow \theta$

Estimate advantage functions $\hat{A}_{i,t}$ and $\hat{A}_{i,t}^C, i = 1, \dots, M, t = 1, \dots, T$ using GAE.

Get $V_{i,t}^{\text{target}} = \hat{A}_{i,t} + V_\phi(s_{i,t})$ and $V_{i,t}^{C,\text{target}} = \hat{A}_{i,t} + V_\psi^C(s_{i,t})$

Update ν by

$$\nu \leftarrow \underset{\nu}{\text{proj}} \left[\nu - \alpha_\nu (b - \hat{J}_C) \right]$$

for K epochs **do**

for each minibatch $\{s_j, a_j, A_j, A_j^C, V_j^{\text{target}}, V_j^{C,\text{target}} : j = 1, \dots, N\}$ of size B selected from the batch data **do**
Value loss functions

$$L_V(\phi) = \frac{1}{2N} \sum_{j=1}^B (V_\phi(s_j) - V_j^{\text{target}})^2$$

$$L_{VC}(\psi) = \frac{1}{2N} \sum_{j=1}^B (V_\psi(s_j) - V_j^{C,\text{target}})^2$$

Update value networks

$$\phi \leftarrow \phi - \alpha_V \nabla_\phi L_V(\phi)$$

$$\psi \leftarrow \psi - \alpha_V \nabla_\psi L_{VC}(\psi)$$

Update policy

$$\theta \leftarrow \theta - \alpha_\pi \hat{\nabla}_\theta \mathcal{L}(\theta)$$

where

$$\hat{\nabla}_\theta \mathcal{L}(\theta) \approx \frac{1}{B} \sum_{j=1}^B \left[\nabla_\theta D_{\text{KL}}(\pi_\theta \| \pi_{\theta'})[s_j] - \frac{1}{\lambda} \frac{\nabla_\theta \pi_\theta(a_j | s_j)}{\pi_{\theta'}(a_j | s_j)} (\hat{A}_j - \nu \hat{A}_j^C) \right] \mathbf{1}_{D_{\text{KL}}(\pi_\theta \| \pi_{\theta'})[s_j] \leq \delta}$$

end for

if $\frac{1}{MT} \sum_{i=1}^M \sum_{t=0}^{T-1} D_{\text{KL}}(\pi_\theta \| \pi_{\theta'})[s_{i,t}] > \delta$ **then**
Break out of inner loop

end if

end for

until stopping criteria met

E. Implementation Details for Experiments

All experiments were implemented in Pytorch 1.3.1 and Python 3.7.4 on Intel Xeon Gold 6230 processors. We used our own Pytorch implementation of CPO based on <https://github.com/jachiam/cpo>. For PPO, PPO Lagrangian, TRPO Lagrangian, we used an optimized PPO and TRPO implementation based on <https://github.com/Khrylx/PyTorch-RL>, <https://github.com/ikostrikov/pytorch-a2c-ppo-acktr-gail>, and <https://github.com/ikostrikov/pytorch-trpo>.

E.1. Robots with Speed Limit

E.1.1. ENVIRONMENT DETAILS

We used the MuJoCo environments provided by OpenAI Gym (Brockman et al., 2016) for this set of experiments. For agents maneuvering on a two-dimensional plane, the cost is calculated as

$$C(s, a) = \sqrt{v_x^2 + v_y^2}$$

For agents moving along a straight line, the cost is calculated as

$$C(s, a) = |v_x|$$

where v_x, v_y are the velocities of the agent in the x and y directions respectively.

E.1.2. ALGORITHMIC HYPERPARAMETERS

We used a two-layer feedforward neural network with a tanh activation for both our policy and value networks. We assume the policy is Gaussian with independent action dimensions. The policy networks outputs a mean vector and a vector containing the state-independent log standard deviations. States are normalized by the running mean the running standard deviation before being fed to any network. The advantage values are normalized by the batch mean and batch standard deviation before being used for policy updates. Except for the learning rate for ν which is kept fixed, all other learning rates are linearly annealed to 0 over the course of training. Table 4 summarizes the hyperparameters used in our experiments.

E.2. Circle

E.2.1. ENVIRONMENT DETAILS

In the circle tasks, the goal is for an agent to move along the circumference of a circle while remaining within a safety region smaller than the radius of the circle. The exact geometry of the task is shown in Figure 3. The reward and cost functions are

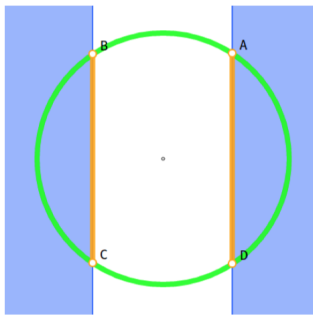


Figure 3. In the Circle task, reward is maximized by moving along the green circle. The agent is not allowed to enter the blue regions, so its optimal constrained path follows the line segments AD and BC (figure and caption taken from (Achiam et al., 2017)).

defined as:

$$R(s) = \frac{-yv_x + xv_y}{1 + |\sqrt{x^2 + y^2} - r|}$$

$$C(s) = \mathbf{1}(|x| > x_{\text{lim}}).$$

Table 4. Hyperparameters for Robots with Speed Limit Experiments

Hyperparameter	PPO	PPO-L	TRPO-L	CPO	FOCOPS
No. of hidden layers	2	2	2	2	2
No. of hidden nodes	64	64	64	64	64
Activation	tanh	tanh	tanh	tanh	tanh
Initial log std	-0.5	-0.5	-0.5	-0.5	-0.5
Discount for reward γ	0.995	0.995	0.995	0.995	0.995
Discount for cost γ_C	0.995	0.995	0.995	0.995	0.995
Batch size	2048	2048	2048	2048	2048
Minibatch size	64	64	N/A	N/A	64
No. of optimization epochs	10	10	N/A	N/A	30
Maximum episode length	1000	1000	1000	1000	1000
GAE parameter (reward)	0.95	0.95	0.95	0.95	0.95
GAE parameter (cost)	N/A	0.95	0.95	0.95	0.95
Learning rate for policy	3×10^{-4}	3×10^{-4}	N/A	N/A	3×10^{-4}
Learning rate for reward value net	3×10^{-4}	3×10^{-4}	3×10^{-4}	3×10^{-4}	3×10^{-4}
Learning rate for cost value net	N/A	3×10^{-4}	3×10^{-4}	3×10^{-4}	3×10^{-4}
Learning rate for ν	N/A	0.01	0.01	N/A	0.01
L_2 -regularization coeff. for value net	3×10^{-3}	3×10^{-3}	3×10^{-3}	3×10^{-3}	3×10^{-3}
Clipping coefficient	0.2	N/A	N/A	N/A	N/A
Damping coeff.	N/A	N/A	0.01	0.01	N/A
Backtracking coeff.	N/A	N/A	0.8	0.8	N/A
Max backtracking iterations	N/A	N/A	10	10	N/A
Max conjugate gradient iterations	N/A	N/A	10	10	N/A
Iterations for training value net ¹	1	1	80	80	1
Temperature λ	N/A	N/A	N/A	N/A	1.3
Trust region bound δ	N/A	N/A	0.01	0.01	0.05
Initial ν, ν_{\max}	N/A	0, 2	0, 2	N/A	0, 2

where x, y are the positions of the agent on the plane, v_x, v_y are the velocities of the agent along the x and y directions, r is the radius of the circle, and x_{lim} specifies the range of the safety region. The radius is set to $r = 10$ for both Ant and Humanoid while x_{lim} is set to 3 and 2.5 for Ant and Humanoid respectively. Note that these settings are identical to those of the circle task in (Achiam et al., 2017). Our experiments were implemented in OpenAI Gym (Brockman et al., 2016) while the circle tasks in (Achiam et al., 2017) were implemented in rllab (Duan et al., 2016). We also excluded the Point agent from the original experiments since it is not a valid agent in OpenAI Gym. The first two dimensions in the state space are the (x, y) coordinates of the center mass of the agent, hence the state space for both agents has two extra dimensions compared to the standard Ant and Humanoid environments from OpenAI Gym.

E.2.2. ALGORITHMIC HYPERPARAMETERS

For these tasks, we used identical settings as the robots with speed limit tasks except we used a batch size of 50000 for all algorithms and a minibatch size of 1000 for PPO, PPO-Lagrangian, and FOCOPS. The discount rate for both reward and cost were set to 0.995. For FOCOPS, we set $\lambda = 1.0$.

E.3. Generalization Analysis

During the training phase, we trained agents using all four algorithms (PPO Lagrangian, TRPO Lagrangian, CPO, and FOCOPS) with 10 different random seeds. For the robots with speed limit tasks the agents were trained for 1 million samples, for the circle tasks, the agents were trained for 10 million samples. For each algorithm, we picked the seed with the highest maximum return of the last 100 episodes which does not violate the cost constraint at the end of training. The

¹for PPO, PPO-L, and FOCOPS, this refers to the number of iteration for training the value net per minibatch update.

First Order Optimization in Policy Space for Constrained Deep Reinforcement Learning

reasoning here is that for a fair comparison, we wish to pick the best performing seed for each algorithm. We then ran 10 episodes using the trained agents on 10 unseen random seeds (identical seeds are used for all four algorithms) to test how well the algorithms generalize over unseen data. The final results of running the trained agents on the speed limit and circle tasks are reported in Tables 5 and 6.

Table 5. Average return of 10 episodes for trained agents on the robots with speed limit tasks on 10 unseen random seeds . The results are normalized using the reward/cost returns of an unconstrained PPO agent. Results shown are the bootstrap mean and normal 95% confidence interval with 1000 bootstrap samples.

Environment		PPO-L	TRPO-L	CPO	FOCOPS
Ant-v3	Reward	0.709 ± 0.013	0.477 ± 0.001	0.566 ± 0.015	0.942 ± 0.006
	Cost	0.353 ± 0.018	0.185 ± 0.023	0.352 ± 0.028	0.526 ± 0.007
HalfCheetah-v3	Reward	0.484 ± 0.039	0.579 ± 0.005	0.693 ± 0.003	0.553 ± 0.004
	Cost	0.544 ± 0.027	0.528 ± 0.011	0.647 ± 0.005	0.545 ± 0.005
Hopper-v3	Reward	1.014 ± 0.003	0.847 ± 0.026	1.246 ± 0.022	1.060 ± 0.034
	Cost	0.505 ± 0.001	0.491 ± 0.001	0.576 ± 0.007	0.494 ± 0.003
Humanoid-v3	Reward	0.812 ± 0.031	0.694 ± 0.022	0.743 ± 0.018	1.024 ± 0.034
	Cost	0.440 ± 0.022	0.524 ± 0.016	0.523 ± 0.017	0.422 ± 0.019
Swimmer-v3	Reward	0.443 ± 0.009	0.436 ± 0.017	0.380 ± 0.034	0.446 ± 0.012
	Cost	0.618 ± 0.008	0.332 ± 0.017	0.253 ± 0.016	0.377 ± 0.016
Walker2d-v3	Reward	0.843 ± 0.187	0.589 ± 0.062	0.841 ± 0.002	1.135 ± 0.051
	Cost	0.450 ± 0.026	0.556 ± 0.007	0.346 ± 0.008	0.452 ± 0.006

Table 6. Average return of 10 episodes for trained agents on the circle tasks on 10 unseen random seeds . The results are normalized using the reward/cost returns of an unconstrained PPO agent. Results shown are the bootstrap mean and normal 95% confidence interval with 1000 bootstrap samples.

Environment		PPO-L	TRPO-L	CPO	FOCOPS
Ant-Circle	Reward	0.085 ± 0.016	0.080 ± 0.014	0.087 ± 0.013	0.120 ± 0.017
	Cost	0.258 ± 0.035	0.240 ± 0.027	0.304 ± 0.034	0.242 ± 0.018
Humanoid-Circle	Reward	0.438 ± 0.062	0.258 ± 0.013	0.227 ± 0.013	0.433 ± 0.044
	Cost	0.358 ± 0.031	0.340 ± 0.030	0.330 ± 0.023	0.343 ± 0.032

For the robots with speed limit tasks, FOCOPS outperforms the other three algorithms on four out of six tasks. We note however that while CPO has a higher return on two of the tasks (HalfCheetah and Hopper), this is achieved at the price of significant cost constraint violation.

E.4. Sensitivity Analysis

We tested FOCOPS across ten different values of λ , and ν_{\max} while keeping all other parameters fixed. We also tested the sensitivity of PPO Lagrangian and TRPO Lagrangian to the parameter ν_{\max} . The (normalized) results on the robots with speed limit tasks are reported in Tables 7-10. A value of zero indicates a negative return. One point to note is that PPO Lagrangian is extremely sensitive to the choice of ν_{\max} .

First Order Optimization in Policy Space for Constrained Deep Reinforcement Learning

Table 7. Performance of FOCOPS for Different λ

λ	Ant-v3		HalfCheetah-v3		Hopper-v3		Humanoid-v3		Swimmer-v3		Walker2d-v3		All Environments	
	Reward	Cost	Reward	Cost	Reward	Cost	Reward	Cost	Reward	Cost	Reward	Cost	Reward	Cost
0.1	0.704	0.497	0.462	0.492	0.881	0.486	0.621	0.498	0.310	0.562	0.522	0.487	0.583	0.504
0.5	0.812	0.496	0.486	0.504	1.025	0.500	0.731	0.498	0.364	0.527	0.812	0.497	0.705	0.504
1.0	0.799	0.499	0.441	0.501	0.892	0.493	0.781	0.505	0.349	0.527	0.671	0.494	0.656	0.503
1.3	0.708	0.493	0.448	0.498	0.947	0.498	0.954	0.511	0.346	0.506	0.716	0.495	0.687	0.500
1.5	0.659	0.494	0.449	0.498	0.975	0.492	0.809	0.482	0.425	0.515	0.671	0.487	0.665	0.495
2.0	0.411	0.478	0.453	0.496	0.996	0.498	0.803	0.504	0.426	0.495	0.532	0.497	0.604	0.495
2.5	0.292	0.449	0.467	0.504	0.493	0.499	0.798	0.509	0.423	0.514	0.550	0.506	0.504	0.497
3.0	0.263	0.457	0.454	0.501	0.904	0.497	0.789	0.489	0.431	0.490	0.585	0.491	0.571	0.488
4.0	0.236	0.440	0.430	0.495	0.918	0.497	0.731	0.499	0.442	0.504	0.526	0.490	0.547	0.488
5.0	0.245	0.428	0.455	0.497	0.894	0.498	0.698	0.505	0.476	0.508	0.589	0.510	0.560	0.491

Table 8. Performance of FOCOPS for Different ν_{\max}

ν_{\max}	Ant-v3		HalfCheetah-v3		Hopper-v3		Humanoid-v3		Swimmer-v3		Walker2d-v3		All Environments	
	Reward	Cost	Reward	Cost	Reward	Cost	Reward	Cost	Reward	Cost	Reward	Cost	Reward	Cost
1	0.735	0.503	0.626	0.612	1.066	0.498	0.954	0.511	0.397	0.622	0.745	0.500	0.754	0.541
2	0.756	0.495	0.468	0.497	0.973	0.497	0.843	0.498	0.353	0.532	0.728	0.489	0.687	0.501
3	0.707	0.491	0.440	0.492	0.947	0.498	0.954	0.511	0.336	0.53	0.718	0.495	0.684	0.503
5	0.707	0.491	0.433	0.495	0.947	0.498	0.954	0.511	0.309	0.503	0.718	0.495	0.678	0.499
10	0.707	0.491	0.433	0.495	0.947	0.498	0.954	0.511	0.338	0.526	0.718	0.495	0.683	0.503
$+\infty$	0.707	0.491	0.433	0.495	0.947	0.498	0.954	0.511	0.348	0.528	0.718	0.495	0.685	0.503

Table 9. Performance of PPO Lagrangian for Different ν_{\max}

ν_{\max}	Ant-v3		HalfCheetah-v3		Hopper-v3		Humanoid-v3		Swimmer-v3		Walker2d-v3		All Environments	
	Reward	Cost	Reward	Cost	Reward	Cost	Reward	Cost	Reward	Cost	Reward	Cost	Reward	Cost
1	0	0.315	0	1.703	0.092	0.551	0.413	0.487	0.504	1.401	0.073	0.523	0.180	0.830
2	0.706	0.489	0.356	0.496	0.812	0.484	0.648	0.498	0.315	0.504	0.721	0.497	0.593	0.495
3	0	0.251	0	1.137	0.266	0.508	0.395	0.477	0.201	0.999	0.061	0.465	0.154	0.640
5	0	0.216	0	1.383	0.265	0.492	0.387	0.479	0	1.650	0.075	0.476	0.121	0.783
10	0	0.276	0	1.632	0.265	0.492	0.387	0.479	0	2.746	0.078	0.478	0.122	1.017
$+\infty$	0	0.279	0	1.149	0.265	0.492	0.387	0.479	0	1.111	0.078	0.478	0.122	0.665

Table 10. Performance of TRPO Lagrangian for Different ν_{\max}

ν_{\max}	Ant-v3		HalfCheetah-v3		Hopper-v3		Humanoid-v3		Swimmer-v3		Walker2d-v3		All Environments	
	Reward	Cost	Reward	Cost	Reward	Cost	Reward	Cost	Reward	Cost	Reward	Cost	Reward	Cost
1	0.713	0.500	0.704	0.679	0.611	0.504	0.680	0.499	0.425	0.608	0.476	0.495	0.608	0.548
2	0.702	0.513	0.502	0.530	0.388	0.529	0.680	0.499	0.334	0.533	0.358	0.502	0.494	0.518
3	0.696	0.507	0.515	0.532	0.414	0.532	0.680	0.499	0.296	0.672	0.347	0.495	0.491	0.540
5	0.696	0.507	0.492	0.523	0.358	0.516	0.680	0.499	0.228	0.670	0.347	0.505	0.467	0.537
10	0.696	0.507	0.478	0.509	0.340	0.519	0.680	0.499	0.308	0.765	0.344	0.497	0.474	0.549
$+\infty$	0.696	0.507	0.475	0.506	0.359	0.518	0.680	0.499	0.303	0.778	0.344	0.497	0.476	0.551